Pulmonary embolism detection on venous thrombosis ultrasound images with bi-dimensional entropy measures: preliminary results

Antoine Jamin, Clément Hoffmann, Guillaume Mahé, Luc Bressollette, Anne Humeau-Heurtier

▶ **To cite this version:**

Antoine Jamin, Clément Hoffmann, Guillaume Mahé, Luc Bressollette, Anne Humeau-Heurtier. Pulmonary embolism detection on venous thrombosis ultrasound images with bi-dimensional entropy measures: preliminary results. Medical Physics, 2023, 50 (12), pp.7840-7851. 10.1002/mp.16568 . hal-04115305

HAL Id: hal-04115305
https://univ-angers.hal.science/hal-04115305v1

Submitted on 23 Jan 2024

HAL is a multi-disciplinary open access archive for the deposit and dissemination of scientific research documents, whether they are published or not. The documents may come from teaching and research institutions in France or abroad, or from public or private research centers.

L'archive ouverte pluridisciplinaire **HAL**, est destinée au dépôt et à la diffusion de documents scientifiques de niveau recherche, publiés ou non, émanant des établissements d'enseignement et de recherche français ou étrangers, des laboratoires publics ou privés.

Distributed under a Creative Commons Attribution 4.0 International License

Check for updates

Received: 24 March 2022 | Revised: 1 June 2023 | Accepted: 1 June 2023

DOI: 10.1002/mp.16568

RESEARCH ARTICLE

MEDICAL PHYSICS

Pulmonary embolism detection on venous thrombosis ultrasound images with bi-dimensional entropy measures: Preliminary results

Antoine Jamin[1] | **Clément Hoffmann**[2,3,4] | **Guillaume Mahe**[5,6,7] | **Luc Bressollette**[2,3,4] | **Anne Humeau-Heurtier**[8]

[1]Univ Angers, LERIA, SFR MATHSTIC, Angers, France

[2]Internal and Vascular Medicine and Pulmonology Department, CHU Brest, Brest, France

[3]INSERM U1304 Groupe d'Etude de la Thrombose de Bretagne Occidentale (GETBO), University Brest, Brest, France

[4]F-CRIN INNOVTE, Saint-Etienne, France

[5]Vascular Medicine Department, Centre Hospitalier Universitaire (CHU) de Rennes, Rennes, France

[6]INSERM CIC1414 CIC Rennes, Rennes, France

[7]Université de Rennes 2, M2S-EA 7470, Rennes, France

[8]Univ Angers, LARIS, SFR MATHSTIC, Angers, France

Correspondence
Antoine JAMIN, Univ Angers, LERIA, SFR MATHSTIC, F-49000 Angers, France.
Email: research@antoine-jamin.fr

Abstract

Background: Venous thromboembolism (VTE) is a common health issue. A clinical expression of VTE is a deep vein thrombosis (DVT) that may lead to pulmonary embolism (PE), a critical illness. When DVT is suspected, an ultrasound exam is performed. However, the characteristics of the clot observed on ultrasound images cannot be linked with the presence of PE. Computed tomography angiography is the gold standard to diagnose PE. Nevertheless, the latter technique is expensive and requires the use of contrast agents.

Purpose: In this article, we present an image processing method based on ultrasound images to determine whether PE is associated or not with lower limb DVT. In terms of medical equipment, this new approach (Doppler ultrasound image processing) is inexpensive and quite easy.

Methods: With the aim to help medical doctors in detecting PE, we herein propose to process ultrasound images of patients with DVT. After a first step based on histogram equalization, the analysis procedure is based on the use of bi-dimensional entropy measures. Two different algorithms are tested: the bi-dimensional dispersion entropy ($DispEn_{2D}$) mesure and the bi-dimensional fuzzy entropy ($FuzEn_{2D}$) mesure. Thirty-two patients (12 women and 20 men, 67.63 ± 16.19 years old), split into two groups (16 with and 16 without PE), compose our database of around 1490 ultrasound images (split into seven different sizes from 32×32 px to 128 × 128 px). *p*-values, computed with the Mann-Whitney test, are used to determine if entropy values of the two groups are statistically significantly different. Receiver operating characteristic (ROC) curves are plotted and analyzed for the most significant cases to define if entropy values are able to discriminate the two groups.

Results: *p*-values show that there are statistical differences between $FuzEn_{2D}$ of patients with PE and patients without PE for 112×112 px and 128×128 px images. Area under the ROC curve (AUC) is higher than 0.7 (threshold for a fair test) for 112× 112 and 128×128 images. The best value of AUC (0.72) is obtained for 112×112 px images.

Conclusions: Bi-dimensional entropy measures applied to ultrasound images seem to offer encouraging perspectives for PE detection: our first experiment, on a small dataset, shows that $FuzEn_{2D}$ on 112×112 px images is able to detect PE. The next step of our work will consist in testing this approach on a larger dataset and in integrating $FuzEn_{2D}$ in a machine learning algorithm. Furthermore, this study could also contribute to PE risk prediction for patients with VTE.

This is an open access article under the terms of the Creative Commons Attribution License, which permits use, distribution and reproduction in any medium, provided the original work is properly cited.

© 2023 The Authors. *Medical Physics* published by Wiley Periodicals LLC on behalf of American Association of Physicists in Medicine.

KEYWORDS
bidimensional entropy, pulmonary embolism, ultrasound images

1 | INTRODUCTION

Venous thromboembolism (VTE) affects around 1 to 2 persons per 1000 each year in the USA.[1] VTE includes deep vein thrombosis (DVT) and pulmonary embolism (PE). The reasons leading to DVT are various: genetic factors, immobilization, surgery, cancer, and idiopathic reasons.[2] PE is the most risky complication for DVT. Early detection and prediction are therefore very important to improve patient care. In case of suspected DVT of the lower limbs, a Doppler ultrasound is performed in order to detect a possible blot clot.[3] Ultrasound images are analyzed by the vascular physician. However, this task can be difficult and tedious. To date, it is not possible to ascertain the presence of PE without performing a computer tomography angiography (CTA) exam. Image processing methods could be an interesting alternative to determine whether PE is associated or not with lower limb DVT.[4]

PE computer-aided diagnosis, through deep learning methods, is often performed from CTA images but, according to a search of the *ScienceDirect* database in December 2022 and based on the keywords "pulmonary embolism" and "ultrasound image", it has not been investigated from any other kinds of images.[5–8] Several studies proposed the use of machine learning methods to analyze ultrasound images (diagnosis of breast lesion, thyroid nodule, liver lesion, etc.) but none of them has focused on PE detection.[9,10] The features studied are often related to texture. Various classifiers can be proposed for these features: linear, Bayesian, support vector machine, artificial neural network, etc.[9] Texture features extraction has recently been performed through the use of bi-dimensional entropy measures.[11–14] The results revealed interesting properties of these entropy values to quantify texture for a variety of images. Because the initial bi-dimensional entropy method, called two-dimensional sample entropy, is not very robust for small images and because it is computationally expensive, two other entropy-based approaches have recently been introduced for texture analysis: bi-dimensional dispersion entropy ($DispEn_{2D}$) and bi-dimensional fuzzy entropy ($FuzEn_{2D}$).[15–17]

In this study, we propose to contribute to the computer-aided diagnosis of PE from ultrasound images of lower limbs. This has never been proposed for PE detection. Ultrasound exams have the advantage of being less expensive and easier to perform than CTA. In our work we analyze the association between PE and thrombus structure of the lower limb DVT. Thirty-two patients suffering from DVT were included in the study (Hospital of Brest, France). Ultrasound images of their blood clot were recorded by a medical expert. Then, regions of interest, that contain only the thrombus, have been extracted from each ultrasound image. Various preprocessing methods have been used to improve the image quality. The images were then processed with two approaches, $DispEn_{2D}$ and $FuzEn_{2D}$, with the aim to differentiate patient with PE from those without.

This paper is organized as follows: in Section 2 we detail the data processed and the methods. Section 3 presents the results for the two approaches: $DispEn_{2D}$ and $FuzEn_{2D}$. In Section 4 we discuss our results. The paper ends with a conclusion.

2 | METHODS

2.1 | Context and population

Data were collected from the University Hospital of Brest, France, on patients with lower limb DVT. For each patient, ultrasound images (at least two) of the blood clot area were recorded by a vascular physician. Three physicians, with at least two years experience in ultrasound acquisition, participated to the study. A Toshiba Aplio 500 using a convex transducer at 5 MHz frequency[4] was used. Thrombus images (saved in DICOM format) were extracted manually from the ultrasound images by the practician with a customized software and were segmented onto different sizes depending on the blood clot size. The outline of the study is presented in Figure 1.

Our database was composed of 32 patients, 12 women and 20 men, 67.63 ± 16.19 years old. For our study, patients were split into two uniform groups: those without PE and those with. Cohorts are detailed in Table 1.

TABLE 1 Cohort details.

	Pulmonary embolism		No pulmonary embolism	
Image size (px)	#images	#patients	#images	#patients
32x32	83	16	85	16
48x48	70	16	71	16
64x64	70	16	70	16
80x80	70	16	70	16
96x96	70	16	70	16
112x112	66	16	67	16
128x128	66	16	66	16

24734209, 2023, 12, Downloaded from https://aapm.onlinelibrary.wiley.com/doi/10.1002/mp.16568 by Cochrane France, Wiley Online Library on [23/01/2024]. See the Terms and Conditions (https://onlinelibrary.wiley.com/terms-and-conditions) on Wiley Online Library for rules of use; OA articles are governed by the applicable Creative Commons License

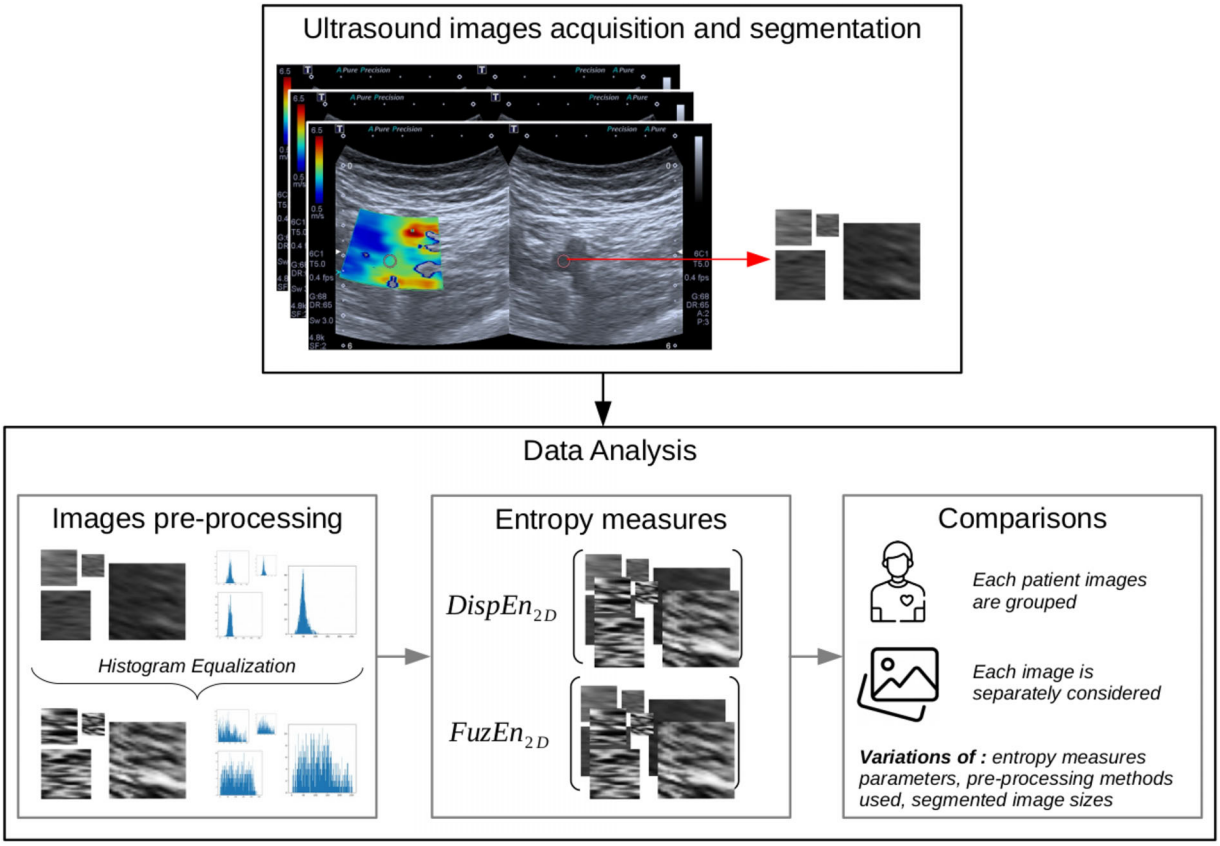

FIGURE 1 Outline of the study. First, ultrasound images (at least two) were recorded from each patient. Secondly, thrombus images, of different sizes, were extracted manually by the vascular physician from the blood clot area located on the ultrasound images. Thirdly, images were pre-processed with histogram equalization methods. Fourthly, bi-dimensional entropy values were computed, with two methods, on all images (pre-processed and source). Finally, these bi-dimensional entropy values were compared in two steps: images were grouped by patient ID, and each image was considered separately.

The association with PE was confirmed following the European Society of Cardiology (ESC) guidelines,[18] with a thoracic computed tomography (CT) scan or a ventilation/perfusion (V/Q) lung scan.

2.2 | Histogram equalization

Because images are very dependent on acquisition methods and parameters, a normalization is often necessary to reduce these dependencies. Image normalization can consist in equalization of image histogram to improve the contrast and to highlight the different elements in the image. In this study, we used three histogram equalization methods: conventional histogram equalization (HE), sorted histogram equalization (SHE), and contrast limited adaptive histogram equalization (CLAHE).

HE transforms an image to adjust its histogram in order to maximize its entropy and image information content. SHE unifies the image histogram considering the pixel locations and values.[19] SHE also gives extra-information, boundary values, because each location and value are stored into a list sorted by pixel values in ascending order. CLAHE is a method that equalizes the image histogram by operating on a small region, rather than on the whole image. It reduces the noise amplification problem, by trimming the histogram to a preset value fixed before computing the cumulative distribution function (uniform, Rayleigh, or exponential).[20] This method is often used on medical images and with low-contrast images.[21]

2.3 | Bi-dimensional dispersion entropy ($DispEn_{2D}$)

To quantify the patterns irregularity of an image, bi-dimensional entropy measures have been introduced.[14] Azami et al. proposed the $DispEn_{2D}$ to overcome two major drawbacks of the two-dimensional sample entropy method: undefined values for small images and computational expensiveness.[15]

$DispEn_{2D}$ of an image, of size $h \times w$, $\mathbf{U} = \{u_{i,j}\}$, is computed as:

24734209, 2023, 12, Downloaded from https://aapm.onlinelibrary.wiley.com/doi/10.1002/mp.16568 by Cochrane France, Wiley Online Library on [23/01/2024]. See the Terms and Conditions (https://onlinelibrary.wiley.com/terms-and-conditions) on Wiley Online Library for rules of use; OA articles are governed by the applicable Creative Commons License

$$DispEn_{2D}(\mathbf{U}, \mathbf{m}, c) = -\sum_{\pi=1}^{c^{m_w \times m_h}} p(\pi_{v_0 \ldots v_{m_w \times m_h}}) \times \ln\left(p(\pi_{v_0 \ldots v_{m_w \times m_h}})\right), \quad (1)$$

where $\mathbf{m} = [m_h, m_w]$ is the embedded dimension vector. c is the number of classes, and $p(\pi_{v_0 \ldots v_{m_w \times m_h}})$ is calculated as:

$$p(\pi_{v_0 \ldots v_{m_h \times m_{w-1}}}) = \frac{\#\left\{k, l \middle| k \leq h - (m_{h-1}), l \leq w - (m_{w-1}), \mathbf{z}_{k,l}^{\mathbf{m},c} \text{ has type } \pi_{v_0 \ldots v_{m_h \times m_{w-1}}}\right\}}{(h - (m_{h-1}))(w - (m_{w-1}))}, \quad (2)$$

where $k = 1, 2, \ldots, w - (m_w - 1)$, $l = 1, 2, \ldots, h - (m_h - 1)$, $\pi_{v_0 \ldots v_{m_w \times m_h}}$ is a dispersion pattern obtained with:

$$\begin{aligned}\mathbf{z}_{k,l}^{\mathbf{m},c} = \{&z_{k,l}^c, z_{k,l+1}^c, \ldots, z_{k,l+(m_w-1)}^c, z_{k+1,l}^c, z_{k+1,l+1}^c, \ldots \\ &\times, z_{k+1,l+(m_w-1)}^c, \ldots, z_{k+(m_h-1),l}^c, z_{k+(m_h-1),l+1}^c, \ldots \\ &\times, z_{k+(m_h-1),l+(m_w-1)}^c\},\end{aligned} \quad (3)$$

where $z_{k,l}^c = v_0$, $z_{k,l+1}^c = v_1$, ..., $z_{k+(m_h-1),l+(m_w-1)}^c = v_{m_h \times m_v - 1}$. $z_{i,j}^c = \text{round}(c \times y_{i,j} + 0.5)$ where $y_{i,j}$ is element of the classes matrix $\mathbf{Y}$ obtained by mapping $\mathbf{U}$ to classes with the normal cumulative distribution function of pixels image from 0 to 1 as follows:

$$y_{i,j} = \frac{1}{\sigma\sqrt{2\pi}} \int_{-\infty}^{x_{i,j}} \exp \frac{-(t-\mu)^2}{2\sigma^2} dt. \quad (4)$$

μ and σ are, respectively, the mean and standard deviation of $\mathbf{U}$.

From the authors' recommendations, $DispEn_{2D}$ parameters should verify the following condition: $(c^{m_h \times m_w}) < ((h - (m_h - 1)) \times (w - (m_w - 1)))$. For this reason and in accordance with the image size of our database, we have considered $m_h = m_w = 2$ and c between 3 to 5.

2.4 | Bi-dimensional fuzzy entropy ($FuzEn_{2D}$)

Hilal et al. proposed $FuzEn_{2D}$ to improve the reliability and results stability of entropy measures obtained with previous methods like bi-dimensional sample entropy.[16,17]

$FuzEn_{2D}$ of an image, of size $h \times w$, $\mathbf{U} = \{u_{i,j}\}$, is computed as:

$$FuzEn_{2D}(\mathbf{U}, \mathbf{m}, n, r) = \ln \frac{\Phi^{\mathbf{m}}(n, r)}{\Phi^{\mathbf{m}+1}(n, r)}, \quad (5)$$

where $\mathbf{m} = [m_h, m_w]$ is the embedded dimension, n is the fuzzy power, r is the tolerance level, and $\Phi^{\mathbf{m}}(n, r)$ is calculated as:

$$\Phi^{\mathbf{m}}(n, r) = \frac{1}{N_{\mathbf{m}}} \sum_{i=1,j=1}^{i=h-m_h, j=w-m_w} \Phi_{i,j}^{\mathbf{m}}(n, r), \quad (6)$$

where $N_{\mathbf{m}} = (w - m_w)(h - m_h)$ and $\Phi_{i,j}^{\mathbf{m}}(n, r)$ is computed as:

$$\Phi_{i,j}^{\mathbf{m}}(n, r) = \frac{1}{N_{\mathbf{m}} - 1} \sum_{a=1,b=1}^{a=h-m_h, b=w-m_w} D_{ij,ab}^{\mathbf{m}}(n, r), \quad (7)$$

where $D_{ij,ab}^{\mathbf{m}}(n, r)$ is calculated as:

$$D_{ij,ab}^{\mathbf{m}}(n, r) = \mu(d_{ij,ab}^{\mathbf{m}}, n, r) = \exp -\frac{(d_{ij,ab}^{\mathbf{m}})^2}{r}, \quad (8)$$

where $\mu(d_{ij,ab}^{\mathbf{m}}, n, r)$ is a fuzzy function and $d_{ij,ab}^{\mathbf{m}}$ is computed as:

$$\begin{aligned}d_{ij,ab}^{\mathbf{m}} = d[\mathbf{X}_{i,j}^{\mathbf{m}}, \mathbf{X}_{a,b}^{\mathbf{m}}] = &\max_{k,l \in (0,\mathbf{m}-1)} |u(i + k, j + l) \\ &- u(a + k, b + l)|,\end{aligned} \quad (9)$$

where $\mathbf{X}_{i,j}^{\mathbf{m}} = \begin{bmatrix} u_{i,j} & \ldots & u_{i,j+\mathbf{m}-1} \\ u_{i+1,j} & \ldots & u_{i+1,j+\mathbf{m}-1} \\ \ldots & \ldots & \ldots \\ u_{i+\mathbf{m}-1,j} & \ldots & u_{i+\mathbf{m}-1,j+\mathbf{m}-1} \end{bmatrix}$.

In accordance with the image size of our database and the results obtained by Hilal et al., we set $m_h = m_w = 2$ in our study.[16,17]

2.5 | Statistical analysis

Figure 2 illustrates the complete statistical analysis process that was led. As mentioned above, each

24734209, 2023, 12, Downloaded from https://aapm.onlinelibrary.wiley.com/doi/10.1002/mp.16568 by Cochrane France, Wiley Online Library on [23/01/2024]. See the Terms and Conditions (https://onlinelibrary.wiley.com/terms-and-conditions) on Wiley Online Library for rules of use; OA articles are governed by the applicable Creative Commons License

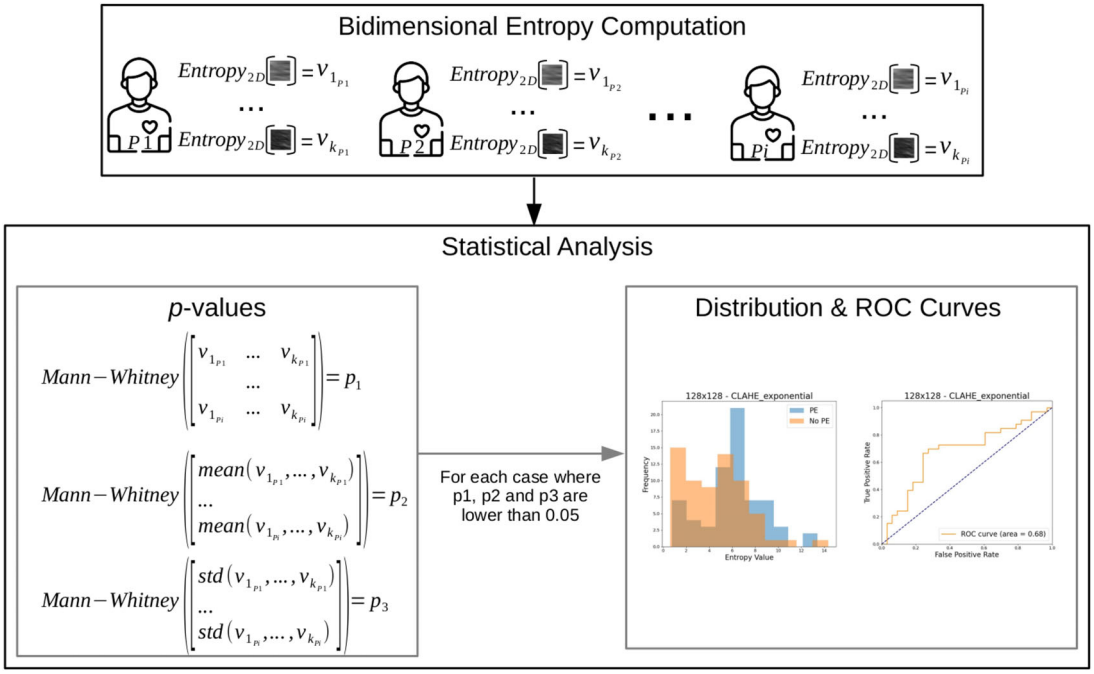

FIGURE 2 Statistical analysis process description. First, 2D entropy values are computed from all images. Then, three *p*-values are calculated with: (1) all entropy values, (2) the mean of entropy values of all patient images, and (3) the standard deviation of entropy values of all patient images. The last two *p*-values are computed to evaluate the impact of the repeatability of the measurement. Finally, for the cases when the three *p*-values are statistically significantly different (*p*-value < 0.05), the distribution and the receiver-operating curves of entropy values are analyzed.

TABLE 2 *p*-values calculated with the Mann-Whitney test by comparing the bidimensional dispersion entropy (with $c = 3$) values of two groups: presence or absence of pulmonary embolism. We considered all the images regardless of the patient ID (*all images* rows). Due to the different numbers of images per patient, we also grouped images per patient ID and we considered the mean and standard deviation of bidimensional dispersion entropy values (*mean* and *std* rows). Statistically significantly different *p*-values are in blue. The three preprocessing methods used are: histogram equalization , sorted histogram equalization, and contrast limited adaptive histogram equalization.

		Image size in pixels						
Preprocessing method	**Cases**	**32×32**	**48×48**	**64×64**	**80×80**	**96×96**	**112×112**	**128×128**
HE	all images	0.422	0.499	0.240	0.102	0.089	0.032	0.002
	mean	0.280	0.267	0.477	0.462	0.433	0.433	0.403
	std	0.243	0.209	0.403	0.492	0.492	0.389	0.280
SHE	all images	0.421	0.198	0.055	0.035	0.026	0.004	$p < 0.001$
	mean	0.477	0.305	0.209	0.220	0.292	0.292	0.209
	std	0.319	0.477	0.319	0.255	0.305	0.188	0.125
CLAHE uniform	all images	0.096	0.061	0.020	0.013	0.020	0.133	0.052
	mean	0.403	0.418	0.374	0.346	0.477	0.374	0.389
	std	0.477	0.448	0.403	0.403	0.477	0.255	0.360
CLAHE rayleigh	all images	0.145	0.102	0.034	0.013	0.020	0.112	0.054
	mean	0.462	0.403	0.389	0.305	0.492	0.360	0.346
	std	0.433	0.292	0.433	0.360	0.418	0.280	0.319
CLAHE exponential	all images	0.131	0.073	0.021	0.010	0.017	0.115	0.043
	mean	0.448	0.389	0.389	0.267	0.492	0.374	0.389
	std	0.492	0.374	0.389	0.374	0.462	0.305	0.389
Without	all images	0.445	0.312	0.157	0.047	0.085	0.031	0.004
	mean	0.292	0.418	0.462	0.462	0.332	0.374	0.477
	std	0.389	0.255	0.477	0.389	0.346	0.492	0.374

Abbreviations: HE, histogram equalization; CLAHE, contrast limited adaptive histogram equalization; SHE, sorted histogram equalization.

24734209, 2023, 12, Downloaded from https://aapm.onlinelibrary.wiley.com/doi/10.1002/mp.16568 by Cochrane France, Wiley Online Library on [23/01/2024]. See the Terms and Conditions (https://onlinelibrary.wiley.com/terms-and-conditions) on Wiley Online Library for rules of use; OA articles are governed by the applicable Creative Commons License

TABLE 3 *p*-values calculated with the Mann-Whitney test by comparing the bidimensional dispersion entropy (with $c = 4$) values of two groups: presence or absence of pulmonary embolism. We considered all the images regardless of the patient ID (*all images* rows). Due to the different numbers of images per patient, we also grouped images per patient ID and we considered the mean and standard deviation of bidimensional dispersion entropy values (*mean* and *std* rows). Statistically significantly different *p*-values are in blue. The three preprocessing methods used are: histogram equalization , sorted histogram equalization , and contrast limited adaptive histogram equalization .

		Image size in pixels						
Preprocessing method	**Cases**	**32×32**	**48×48**	**64×64**	**80×80**	**96×96**	**112×112**	**128×128**
HE	all images	0.379	0.446	0.211	0.079	0.115	0.044	0.003
	mean	0.209	0.267	0.462	0.477	0.462	0.360	0.418
	std	0.198	0.150	0.477	0.477	0.462	0.433	0.280
SHE	all images	0.458	0.178	0.056	0.028	0.029	0.009	$p < 0.001$
	mean	0.492	0.231	0.141	0.178	0.280	0.319	0.231
	std	0.346	0.448	0.243	0.280	0.332	0.231	0.159
CLAHE uniform	all images	0.123	0.127	0.022	0.019	0.023	0.125	0.045
	mean	0.403	0.403	0.433	0.433	0.492	0.389	0.403
	std	0.492	0.389	0.360	0.389	0.492	0.305	0.403
CLAHE rayleigh	all images	0.135	0.119	0.030	0.012	0.014	0.084	0.033
	mean	0.418	0.389	0.477	0.360	0.433	0.374	0.374
	std	0.492	0.360	0.433	0.403	0.462	0.292	0.360
CLAHE exponential	all images	0.116	0.090	0.020	0.015	0.018	0.111	0.040
	mean	0.403	0.389	0.389	0.332	0.477	0.403	0.418
	std	0.462	0.346	0.360	0.374	0.492	0.305	0.433
Without	all images	0.468	0.285	0.109	0.042	0.047	0.035	0.004
	mean	0.267	0.477	0.477	0.492	0.433	0.305	0.492
	std	0.332	0.305	0.448	0.433	0.492	0.418	0.418

Abbreviations: HE, histogram equalization; CLAHE, contrast limited adaptive histogram equalization; SHE, sorted histogram equalization.

pre-processing step (HE, SHE, CLAHE) has been considered separately. Moreover, two bi-dimensional entropy methods, computed with different parameters, have been tested: $DispEn_{2D}$ and $FuzEn_{2D}$. Then, we performed our analysis in two steps. First, we considered the bi-dimensional entropy value of each image regardless of the patient ID (all images). Due to the different number of images per patient we also considered, in a second step, the mean and the standard deviation (std) of the bi-dimensional entropy values for each patient. This latter step was used to evaluate the impact of the repeatability of the measurement. Each image size and each pre-processing method was analyzed separately. To differentiate the two groups (presence or absence of PE), we used the Mann-Whitney test on the bi-dimensional entropy measures and studied the *p*-values. A statistical significance was defined for *p*-values strictly lower than 0.05. The entropy ability to distinguish images of patient with PE from those without was statistically granted when the *p*-values were lower than 0.05 for entropy values of all images, and also for the mean and standard deviation of entropy values for each patient.

An additional two-step statistical analysis has been performed for cases where the *p*-value was lower than 0.05. First, the entropy value distributions were studied. Then, the receiver operating characteristic (ROC) curve was analyzed. The area under the ROC curve (AUC) was calculated to quantify the overall aptitude of a test to discriminate between two outcomes.[22] A fair test was defined for AUC strictly higher than 0.7.

3 | RESULTS

Table 2 shows that $DispEn_{2D}$ values, obtained with $c = 3$, are statistically significantly different (*p*-values ≤ 0.047), between the two groups of subjects, when images are considered regardless of the patient ID. These statistical significant differences are obtained for some image sizes and for some pre-processing methods (64× 64 px: CLAHE; 80 ×80 px: SHE, CLAHE, and Without; 96×96 px: SHE and CLAHE; 112×112 px: HE, SHE, and Without; 128×128 px: HE, SHE, CLAHE exponential, and Without).

Table 3 shows that $DispEn_{2D}$ values, computed with $c = 4$, are statistically significantly different (*p*-values ≤ 0.047), between the two groups of subjects, when images are considered regardless of the patient ID. For image sizes between 32 × 32 px and 112 ×112 px, results are similar to Table 2. For 128×128 px images,

24734209, 2023, 12, Downloaded from https://aapm.onlinelibrary.wiley.com/doi/10.1002/mp.16568 by Cochrane France, Wiley Online Library on [23/01/2024]. See the Terms and Conditions (https://onlinelibrary.wiley.com/terms-and-conditions) on Wiley Online Library for rules of use; OA articles are governed by the applicable Creative Commons License

TABLE 4 *p*-values calculated with the Mann-Whitney test by comparing the bidimensional dispersion entropy (with $c = 5$) values of two groups: presence or absence of pulmonary embolism. We considered all the images regardless of the patient ID (*all images* rows). Due to the different numbers of images per patient, we also grouped images per patient ID and we considered the mean and standard deviation of bidimensional dispersion entropy values (*mean* and *std* rows). Statistically significantly different *p*-values are in blue. The three preprocessing methods used are: histogram equalization , sorted histogram equalization , and contrast limited adaptive histogram equalization .

		Image size in pixels						
Preprocessing method	**Cases**	**32×32**	**48×48**	**64×64**	**80×80**	**96×96**	**112×112**	**128×128**
HE	all images	0.482	0.361	0.185	0.064	0.098	0.053	0.004
	mean	0.292	0.305	0.433	0.492	0.418	0.305	0.448
	std	0.305	0.188	0.448	0.418	0.492	0.448	0.267
SHE	all images	0.497	0.228	0.051	0.032	0.036	0.012	$p < 0.001$
	mean	0.462	0.267	0.141	0.141	0.280	0.389	0.243
	std	0.418	0.477	0.188	0.231	0.319	0.267	0.125
CLAHE uniform	all images	0.118	0.115	0.022	0.021	0.024	0.122	0.047
	mean	0.418	0.418	0.448	0.403	0.448	0.389	0.360
	std	0.462	0.346	0.374	0.374	0.492	0.305	0.332
CLAHE rayleigh	all images	0.158	0.102	0.029	0.017	0.021	0.106	0.040
	mean	0.448	0.418	0.462	0.403	0.492	0.360	0.346
	std	0.492	0.389	0.462	0.374	0.492	0.280	0.346
CLAHE exponential	all images	0.141	0.099	0.018	0.016	0.020	0.111	0.042
	mean	0.448	0.389	0.418	0.389	0.462	0.403	0.418
	std	0.492	0.360	0.346	0.332	0.492	0.346	0.448
Without	all images	0.455	0.261	0.103	0.045	0.034	0.009	0.002
	mean	0.280	0.462	0.462	0.477	0.418	0.403	0.418
	std	0.267	0.346	0.492	0.403	0.477	0.492	0.448

Abbreviations: HE, histogram equalization; CLAHE, contrast limited adaptive histogram equalization; SHE, sorted histogram equalization.

all preprocessing methods lead to statistically significant different $DispEn_{2D}$ values between the two groups (p-values ≤ 0.045).

Table 4 shows, for all image sizes except 112×112 px, similar results to Table 3. For 112×112 px images, $DispEn_{2D}$ values, computed with $c = 5$, are statistically significantly different (p-values ≤ 0.012), between the two groups, without pre-processing method and with SHA, only when images are considered regardless of the patient ID.

Table 5 shows that $FuzEn_{2D}$ values are statistically significantly different (p-values ≤ 0.049), between the two groups of subjects, only when images are considered regardless of the patient ID in these cases:

- 32×32 px: HE, CLAHE Rayleigh;
- 48×48 px: HE, CLAHE uniform and exponential, and Without;
- 64×64 px: HE, SHE, CLAHE exponential, and Without;
- 80×80 px: HE, CLAHE and Without;
- 96×96 px: HE, CLAHE and Without;
- 112×112 px: HE;
- 128×128 px: HE, CLAHE Rayleigh.

The measure repetition does not impact the entropy measure when values in the three comparison cases (all images, mean, and std) are statistically significantly different (p-values ≤ 0.040). Table 5 shows that the measurement repetition does not impact the values in these cases:

- 112×112 px: CLAHE, and Without;
- 128×128 px: CLAHE uniform and exponential, and Without.

The results show that $DispEn_{2D}$, whatever the value of c, is very sensitive to the measurement repetition, the pre-processing method, and the image size. They also show that $FuzEn_{2D}$ is very sensitive to the image size. However, with the largest images (112×112 px and 128×128 px) $FuzEn_{2D}$ is less sensitive to the pre-processing method and to the measurement repetition.

$FuzEn_{2D}$, computed on ultrasound images (112×112 px and 128×128 px) of thrombus with CLAHE or without, seems to be able to differentiate patients with PE and those without. However, p-values are lower with CLAHE uniform for 112×112 px images and without pre-processing for 128×128 px images.

24734209, 2023, 12, Downloaded from https://aapm.onlinelibrary.wiley.com/doi/10.1002/mp.16568 by Cochrane France, Wiley Online Library on [23/01/2024]. See the Terms and Conditions (https://onlinelibrary.wiley.com/terms-and-conditions) on Wiley Online Library for rules of use; OA articles are governed by the applicable Creative Commons License

TABLE 5 *p*-values calculated with the Mann-Whitney test by comparing the bidimensional fuzzy entropy values of two groups: presence or absence of pulmonary embolism. We considered all the images regardless of the patient ID (*all images* rows). Due to the different numbers of images per patient, we also grouped images per patient ID and we considered the mean and standard deviation of bidimensional fuzzy entropy values (*mean* and *std* rows). Statistically significantly different *p*-values are in blue. The three preprocessing methods used are: histogram equalization, sorted histogram equalization, and contrast limited adaptive histogram equalization.

		Image size in pixels						
Preprocessing method	**Cases**	**32×32**	**48×48**	**64×64**	**80×80**	**96×96**	**112×112**	**128×128**
HE	all images	0.049	0.003	0.001	0.001	0.007	0.002	$p < 0.001$
	mean	0.079	0.097	0.073	0.068	0.133	0.125	0.103
	std	0.133	0.118	0.064	0.073	0.073	0.040	0.073
SHE	all images	0.314	0.102	0.024	0.181	0.493	0.301	0.183
	mean	0.360	0.477	0.110	0.332	0.188	0.403	0.418
	std	0.255	0.292	0.068	0.492	0.209	0.292	0.492
CLAHE uniform	all images	0.055	0.022	0.078	0.045	0.019	$p < 0.001$	$p < 0.001$
	mean	0.141	0.267	0.360	0.418	0.492	0.024	0.017
	std	0.097	0.141	0.280	0.346	0.220	0.009	0.017
CLAHE rayleigh	all images	0.041	0.067	0.108	0.003	0.026	0.002	0.001
	mean	0.188	0.492	0.462	0.103	0.360	0.031	0.040
	std	0.231	0.374	0.492	0.103	0.280	0.037	0.079
CLAHE exponential	all images	0.063	0.009	0.034	0.002	0.012	$p < 0.001$	$p < 0.001$
	mean	0.231	0.168	0.292	0.040	0.243	0.026	0.026
	std	0.255	0.141	0.346	0.079	0.231	0.013	0.020
Without	all images	0.0652	0.022	0.037	0.003	0.002	$p < 0.001$	$p < 0.001$
	mean	0.220	0.448	0.492	0.255	0.243	0.037	0.047
	std	0.198	0.360	0.492	0.133	0.118	0.013	0.047

Abbreviations: HE, histogram equalization; CLAHE, contrast limited adaptive histogram equalization; SHE, sorted histogram equalization.

Figure 3 shows the distributions of entropy values for the six cases where *p*-values are statistically significantly different. The entropy values of images from PE patient are higher than those of images from patients without PE. However, the distributions almost overlap.

Figure 4 shows ROC curves generated for the six cases where *p*-values are statistically significantly different (*p*-values ≤ 0.040). AUC is higher than 0.7 only for 112×112 images. The best value of AUC is obtained for 112×112 px images with the CLAHE exponential preprocessing method. $FuzEn_{2D}$ computed on 112×112 px images with CLAHE exponential should therefore be able to distinguish patients with PE from those without.

4 | DISCUSSION

We herein proposed the use of two bi-dimensional entropy measures, $DispEn_{2D}$ and $FuzEn_{2D}$, to determine whether PE is associated or not with lower limb DVT.

Our results (cf. Table 5) show that $FuzEn_{2D}$ values are statistically significantly different (*p*-values $\leq$ 0.040) between patients with PE and those without for 112×112 px and 128×128 px images with CLAHE preprocessing methods (except for Rayleigh) or without pre-processing. Moreover, the ROC curve analysis (cf. Figure 4) shows that $FuzEn_{2D}$ computed on 112×112 px images, pre-processed with CLAHE exponential method, should be able to distinguish patients with PE.

The novelty of our work relies on two main aspects:

- the bi-dimensional entropy measures proposed in our work have never been used to quantify the irregularity (texture) of ultrasound images recorded at the lower limb level. We show here that the texture of lower limb ultrasound images can be studied through bi-dimensional entropy measures.
- The bi-dimensional entropy measures have never been tested to diagnose PE.

Therefore, the novelty of our work not only relies on the scientific aspects (new measure to quantify the texture of lower limb ultrasound images) but also on the medical application.

The two tested entropy measures have drawbacks and advantages. Thus, the algorithms used are rather simple. However, in our study, $DispEn_{2D}$ (cf. Tables 2–4) is not able to differentiate patients with PE from those without: the entropy value is impacted by the repetition measure and the *p*-values computed on mean and

24734209, 2023, 12, Downloaded from https://aapm.onlinelibrary.wiley.com/doi/10.1002/mp.16568 by Cochrane France, Wiley Online Library on [23/01/2024]. See the Terms and Conditions (https://onlinelibrary.wiley.com/terms-and-conditions) on Wiley Online Library for rules of use; OA articles are governed by the applicable Creative Commons License

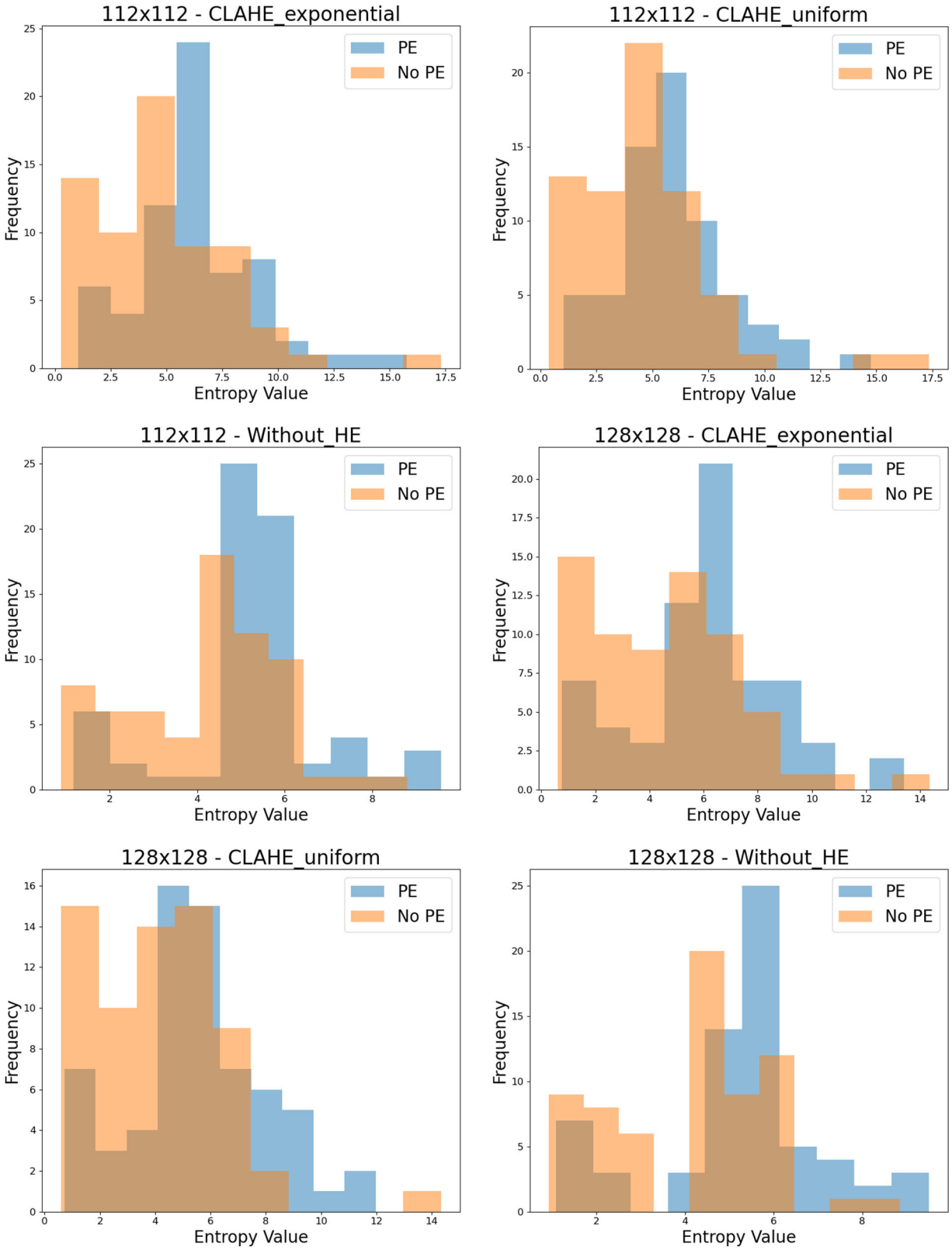

FIGURE 3 Entropy value distributions from the six cases where *p*-values, detailed on Tables 2–5, show statistically significantly differences (*p*-values ≤ 0.040; entropy method: $FuzEn_{2D}$; image sizes: 112×112 px and 128×128 px; pre-processing methods: CLAHE exponential, CLAHE uniform, and without). CLAHE; contrast limited adaptive histogram equalization.

24734209, 2023, 12, Downloaded from https://aapm.onlinelibrary.wiley.com/doi/10.1002/mp.16568 by Cochrane France, Wiley Online Library on [23/01/2024]. See the Terms and Conditions (https://onlinelibrary.wiley.com/terms-and-conditions) on Wiley Online Library for rules of use; OA articles are governed by the applicable Creative Commons License

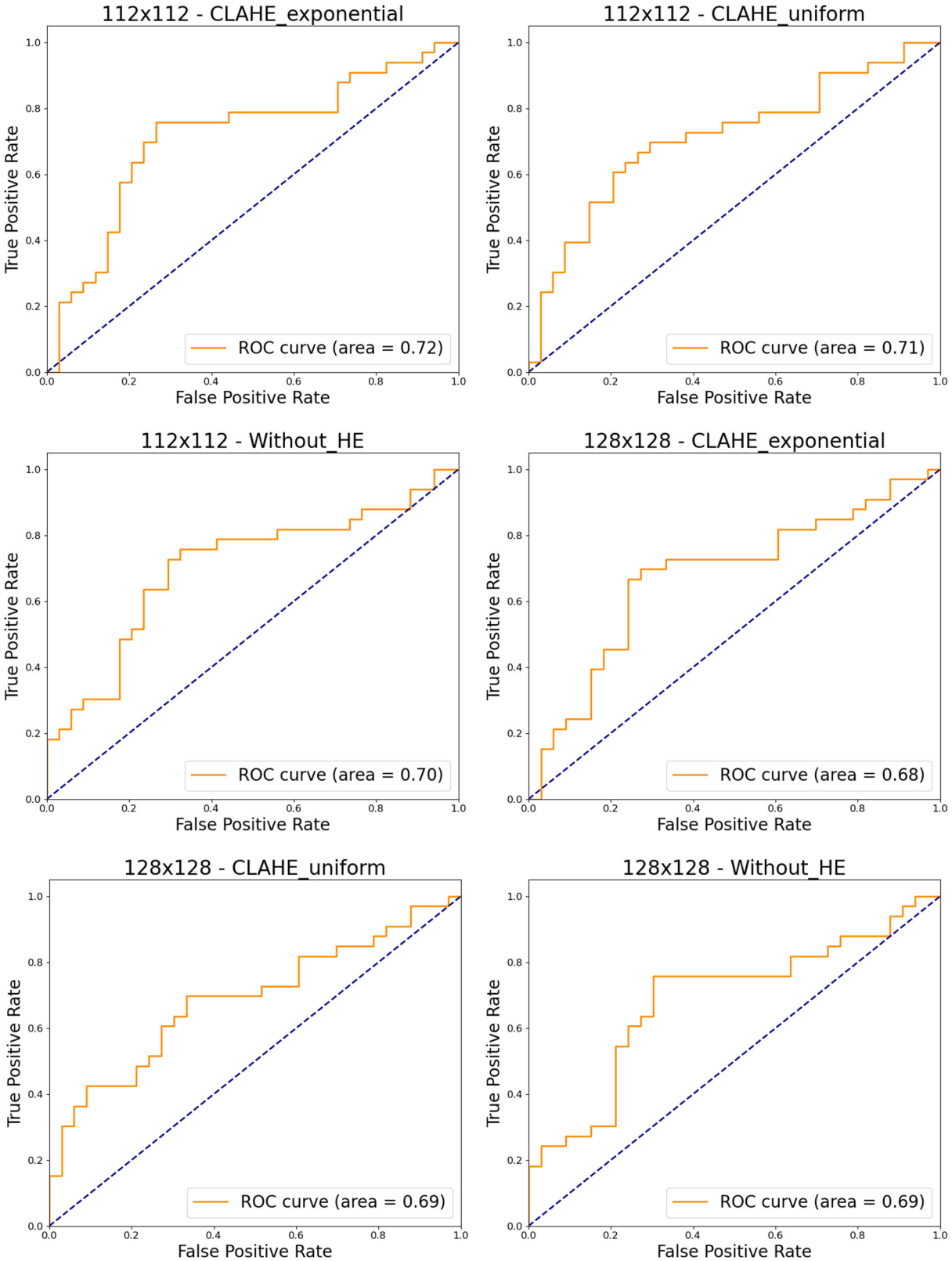

FIGURE 4 ROC curves generated from the six cases where *p*-values, detailed on Tables 2–5, show statistically significantly differences (*p*-values ≤ 0.040; entropy method: $FuzEn_{2D}$; image sizes: 112×112 px and 128×128 px; pre-processing methods: CLAHE exponential, CLAHE uniform, and without). CLAHE; contrast limited adaptive histogram equalization; ROC; Receiver operating characteristic.

24734209, 2023, 12, Downloaded from https://aapm.onlinelibrary.wiley.com/doi/10.1002/mp.16568 by Cochrane France, Wiley Online Library on [23/01/2024]. See the Terms and Conditions (https://onlinelibrary.wiley.com/terms-and-conditions) on Wiley Online Library for rules of use; OA articles are governed by the applicable Creative Commons License

standard deviation entropy values for each patient are larger than 0.05. $FuzEn_{2D}$ is able to split the two groups of patients, without using any pre-processing method. Nevertheless, due to the proximity of the AUC to the minimum acceptability threshold, our method has now to be tested on a larger dataset. Studies that use CTA (gold standard) lead to AUC between 0.85 and 0.95 (cf. Table 1 in Soffer et al. (2021) [7]). Another drawback is that the computation of the two entropy methods tested can be time-consuming for large images and parameter values have to be set. The latter task may not be always simple.[15,17]

The distributions of entropy values (cf. Figure 3) show that the presence of PE may increase some entropy values in ultrasound images. Because the repeatability of pixel patterns is related to the texture properties of images, our results illustrate that PE might impact the texture (image irregularity), quantified by $FuzEn_{2D}$, of lower limb ultrasound images. The ability of $FuzEn_{2D}$ to detect PE through ultrasound images may thus become possible.

The generalizability and the robustness of our approach still has to be tested on a large dataset. However, we can already note that: (i) The pre-processing methods are robust for low-contrast images such as ultrasound images;[21] (ii) The interesting results obtained by bi-dimensional entropy measures when applied on different kinds of medical images lead us to believe that our future results (on a larger dataset) could be promising;[11–17] (iii) Our method relies on pixel values only. This offers good perspectives for generalization.

These preliminary results offer interesting perspectives to detect PE with a less expensive method (ultrasound images of lower limbs) than the existing one (CTA). $FuzEn_{2D}$ values might be calculated during the ultrasound image acquisition to analyze the probability of PE presence.

To improve our method, we could integrate, with a larger dataset, the ultrasound image $FuzEn_{2D}$ values as features in a machine learning algorithm, in relation with previous studies.[23,24] It could also be interesting to analyze if these new features, combined with others, could predict the cause of DVT or estimate the risk of recurrence.

5 | CONCLUSION

In this paper we used two different bi-dimensional entropy-based measures ($DispEn_{2D}$ and $FuzEn_{2D}$) to quantify the texture of ultrasound images. This allowed to distinguish two patient groups: patients with PE and those without. These results are encouraging and offer good perspectives with the aim to predict DVT causes. However, an external validation using a larger cohort is needed. The next step of our work will also be the integration of $FuzEn_{2D}$ values as features in a machine learning algorithm.

ACKNOWLEDGMENTS

Open access funding provided by University of Angers.

CONFLICT OF INTEREST STATEMENT

The authors declare no conflict of interest.

REFERENCES

1. Ortel TL, Neumann I, Ageno W, et al. American Society of Hematology 2020 guidelines for management of venous thromboembolism: treatment of deep vein thrombosis and pulmonary embolism. *Blood Adv*. 2020;4:4693-4738.
2. Nisio MD, van Es N, Büller HR. Deep vein thrombosis and pulmonary embolism. *Lancet*. 2016 Dec 17; 388(10063):3060-3073.
3. Goldhaber SZ, Bounameaux H. Pulmonary embolism and deep vein thrombosis. *Lancet*. 2012 May 12; 379(9828):1835-1846.
4. Berthomier T, Mansour A, Bressollette L, Roy FL, Mottier D. Deep Venous Thrombosis: Database creation and image preprocessing. In: 2016 2nd International Conference on Frontiers of Signal Processing (ICFSP); 2016:87-92.
5. Yang X, Lin Y, Su J, et al. A Two-Stage Convolutional Neural Network for Pulmonary Embolism Detection From CTPA Images. In: IEEE Access. Vol 7. IEEE; 84849-84857.
6. Huang S-C, Pareek A, Zamanian R, Banerjee I, Lungren MP. Multimodal fusion with deep neural networks for leveraging CT imaging and electronic health record: a case-study in pulmonary embolism detection. *Sci Rep*. 2020;10:22147.
7. Soffer S, Klang E, Shimon O, et al. Deep learning for pulmonary embolism detection on computed tomography pulmonary angiogram: a systematic review and meta-analysis. *Sci Rep*. 2021;11(1):15814.
8. Long K, Tang L, Pu X, et al. Probability-based Mask R-CNN for pulmonary embolism detection. *Neurocomputing*. 2021;422:345-353.
9. Huang Q, Zhang F, Li X. Machine Learning in ultrasound computer-aided diagnostic systems: a survey. *Biomed Res Int*. 2018;2018:e5137904.
10. Brattain LJ, Telfer BA, Dhyani M, Grajo JR, Samir AE. Machine learning for medical ultrasound: status, methods, and future opportunities. *Abdom Radiol*. 2018;43:786-799.
11. Moore CJ. A Threshold structure metric for medical image interrogation: the 2d extension of approximate entropy. In: 2016 20th International Conference Information Visualisation (IV). IEEE; 2016:336-341.
12. Humeau-Heurtier A, Mieko Omoto AC, Silva LEV. Bi-dimensional multiscale entropy: relation with discrete Fourier transform and biomedical application. *Comput Biol Med*. 2018;100:36-40.
13. Segato dos Santos LF, Neves LA, Rozendo GB, Ribeiro MG, Zanchetta do Nascimento M, Azevedo Tosta TA. Multidimensional and fuzzy sample entropy (SampEnMF) for quantifying H&E histological images of colorectal cancer. *Comput Biol Med*. 2018;103:148-160.
14. Humeau-Heurtier A. Texture feature extraction methods: a survey. In: *IEEE Access*. IEEE; 2019;7:8975-9000.
15. Azami H, da Silva LEV, Mieko Omoto AC, Humeau-Heurtier A. Two-dimensional dispersion entropy: an information-theoretic method for irregularity analysis of images. *Signal Process Image Commun*. 2019;75:178-187.
16. Hilal M, Humeau-Heurtier A. Bidimensional fuzzy entropy: principle analysis and biomedical applications. In: 2019 41st Annual International Conference of the IEEE Engineering in Medicine and Biology Society (EMBC). IEEE; 2019:4811-4814.
17. Hilal M, Berthin C, Martin L, Azami H, Humeau-Heurtier A. Bidimensional multiscale fuzzy entropy and its application to

24734209, 2023, 12, Downloaded from https://aapm.onlinelibrary.wiley.com/doi/10.1002/mp.16568 by Cochrane France, Wiley Online Library on [23/01/2024]. See the Terms and Conditions (https://onlinelibrary.wiley.com/terms-and-conditions) on Wiley Online Library for rules of use; OA articles are governed by the applicable Creative Commons License

pseudoxanthoma elasticum. *IEEE Trans Biomed Eng*. 2020;67:2015-2022.
18. Konstantinides SV, Torbicki A, Agnelli G, et al. 2014 ESC guidelines on the diagnosis and management of acute pulmonary embolism. *Eur Heart J*. 2014;35:3069a–3069k.
19. Jung I-L, Kim C-S. Image enhancement using sorted histogram specification and POCS postprocessing. In: 2007 IEEE International Conference on Image Processing, Vol 1. IEEE; 2007:2381-8549.
20. Zuiderveld K. Contrast limited adaptive histogram equalization. In: *Graphics gems IV*. Academic Press Professional, Inc.; 1994:474-485.
21. Cernadas E, Fernández-Delgado M, González-Rufino E, Carrión P. Influence of normalization and color space to color texture classification. *Pattern Recognit*. 2017;61:120-138.
22. Carter JV, Pan J, Rai SN, Galandiuk S. ROC-ing along: Evaluation and interpretation of receiver operating characteristic curves. *Surgery*. 2016;159(6):1638-1645.
23. Berthomier T, Mansour A, Bressollette L, Le Roy F, Mottier D. Venous blood clot structure characterization using scattering operator. In: 2016 2nd International Conference on Frontiers of Signal Processing (ICFSP). IEEE; 2016:73-80.
24. Berthomier T, Mansour A, Bressollette L, Le Roy F, Mottier D. Deep venous thrombus characterization: ultrasonography, elastography and scattering operator. *Adv Sci Technol Eng Syst J*. 2017;2:48-59.

How to cite this article: Jamin A, Hoffmann C, Mahe G, Bressollette L, Humeau-Heurtier A. Pulmonary embolism detection on venous thrombosis ultrasound images with bi-dimensional entropy measures: Preliminary results. *Med Phys*. 2023;50:7840–7851. https://doi.org/10.1002/mp.16568

24734209, 2023, 12, Downloaded from https://aapm.onlinelibrary.wiley.com/doi/10.1002/mp.16568 by Cochrane France, Wiley Online Library on [23/01/2024]. See the Terms and Conditions (https://onlinelibrary.wiley.com/terms-and-conditions) on Wiley Online Library for rules of use; OA articles are governed by the applicable Creative Commons License